Microsyst Technol (2017) 23:929–933
DOI 10.1007/s00542-016-2982-4

CrossMark

TECHNICAL PAPER

Investigations of silicon wafer bonding utilizing sputtered Al and Sn films

Zhiyuan Zhu[1,2] · Min Yu[1] · Yufeng Jin[1]

Received: 15 September 2015 / Accepted: 10 May 2016 / Published online: 6 June 2016
© Springer-Verlag Berlin Heidelberg 2016

Abstract Nowadays, wafer bonding is becoming a key enabling technology for three-dimensional (3D) packaging, micro-electro-mechanical systems (MEMS) encapsulation and heterogeneous integration. This paper develops and investigates entire Si wafer bonding based on thin Al and Sn films. 500 nm-thick Al and 500 nm-thick Sn films are sputtered onto silicon wafers. At bonding temperature of 280 °C, the average shear strength of 11 MPa is achieved at bonding time of 1 min. The dependence of shear strength and fracture surface morphology on bonding temperature and bonding time is illustrated. The physical mechanism is proposed. It indicates that high bonding strength can be achieved at appropriate low bonding temperature with proper short bonding time.

1 Introduction

In recent years, metallic wafer bonding has become a key enabling technology in three-dimensional (3D) packaging and heterogeneous integration for providing electrical interconnection and thermal path (Lapisa et al. 2011; Lin et al. 2002; Tana et al. 2012). Metallic wafer bonding is also applied to encapsulate MEMS device and achieve hermetic sealing (Chanchani et al. 2011; Fischer et al. 2012). The total cost can be reduced effectively by packaging devices at wafer level (Saha et al. 2013).

Recently, Al-based wafer bonding technology has been presented and studied. Such technology has advantages of non-sensitivity to wafer surface oxide, compatibility with silicon IC industry, and high electrical and thermal conductivity. Lin et al. (2008) demonstrated that hybrid SiO_2 bonding with Al contact embedded in the SiO_2 to realize electrical interconnections between MEMS and CMOS devices on each bonded wafer. The mechanical support and electrical interconnection are provided by SiO_2 bonding and Al contact, respectively, in this case. The process requires extra chemical mechanical polishing (CMP) to create Al and oxide coplanar surfaces for the subsequent bonding process. The obtained bonding structure may suffer from electrical conduction failure due to the gap between the bottom and top Al layers caused by Al dishing during CMP.

Al-to-Al direct bonding is established to provide both mechanical support and electrical interconnections, where the critical limitation is the native Al oxide that prevents Al-to-Al bonding. Yun et al. (2008) demonstrated Al-to-Al direct bonding at 450 °C with large bonding force up to 80 kN. Malik et al. (2014, 2015) further investigated Al-to-Al direct bonding with varying bonding temperature of 400, 450, 550 °C and force of 18, 36 and 60 kN. The results showed that the bonding strength increased with increasing bonding temperature and bonding force. Although significant progresses have been achieved, major efforts are still needed to achieve Al-to-Al bonding at less harsh bonding conditions.

Al-to-Al wafer bonding with intermediate Sn layer is proposed with advantages of low bonding temperature, low bonding pressure, and short bonding time in comparison with Al-to-Al direct bonding. Therefore, it can reduce

✉ Min Yu
yum@pku.edu.cn

1 National Key Laboratory of Science and Technology on Micro/Nano Fabrication, Institute of Microelectronics, Peking University, No. 5 Yiheyuan Road Haidian District, Beijing 100871, People's Republic of China

2 School of Chemical and Biomolecular Engineering, Georgia Institute of Technology, Atlanta, GA, USA

damage to the functional devices on the bonded silicon wafer. Chang and Lin (2010) reported Sn intermediate layer bonding based on electroplated Al bonding ring for MEMS packaging applications. Zhu et al. (2013) developed full wafer bonding of Al-coated silicon wafer with 2 µm-thick bonding layer and the highest average bonding strength of 9.9 MPa is achieved. It should also be noticed that the bonding process still remains to be intensively investigated to determine the impact of bonding temperature and bonding time on bonding strength. Further, the physical mechanism of intermediate Sn layer bonding needs to be clarified.

In this paper, the dependence of bonding strength on bonding temperature and bonding time is investigated for Al-to-Al wafer bonding with intermediate Sn layer. Scanning electron microscope (SEM) morphologies of fractured surface corresponding with the shear strength of different bonding conditions are analyzed. The physical mechanism for Sn layer bonding is also proposed. It indicates that high bonding strength can be achieved at appropriate low bonding temperature with proper short bonding time. At bonding temperature of 280 °C, the average shear strength of 11 MPa is achieved at bonding time of 1 min.

2 Experimental

In this experiment, we used 4-inch n-type (100) polished wafers with a thickness of 505-545 µm and a resistivity of 2–4 Ω cm. In order to remove organic particles, the bare Si wafers were wet cleaned in H_2SO_4:H_2O_2 (4:1) at 120 °C for 10 min. A 500 nm-thick aluminum layer was sputtered onto the wafers. The wafers were annealed in N_2 ambient (450 °C) for 30 min to form solid adhesion between aluminum and silicon. The in situ Ar plasma sputter cleaning was performed to remove native aluminum oxide so as to ensure good adhesion between aluminum layer and tin layer. Then, a 500 nm-thick tin layer was sputtered onto aluminum layer in the same vacuum chamber.

After that, in an EVG501 bonder, two Si wafers were stacked. The wafers were pressed together at a pressure of 0.25 MPa in vacuum and heated to the bonding temperature. After bonding was finished, the bonded wafers were taken out from wafer bonder at 200 °C which is below the melting point of Sn. As shown in Table 1, the bonding conditions applied in this paper are summarized. The bonding temperatures applied here are higher than the melting point of Sn. The bonded wafers were diced into 5 mm × 5 mm dies for testing.

Then, a Dage Series 4000 shear machine was used to measure the shear strength to debond the bonded dies for the purpose of evaluating bonding strength. The die was clamped to a substrate while a lateral force was applied to the upper side of the bonded die until the specimen was broken. The force at the failure of the sample was recorded.

Table 1 Process parameters of bonding experiments

Experiment no.	Bonding temperature (°C)	Bonding time (min)
1	280	1
2	280	3
3	330	3
4	380	3
5	280	20
6	280	50

After the shear test, the fractured surface was examined by optical microscope, SEM and energy dispersive X-ray spectroscopy (EDS) so as to investigate the physical mechanism.

3 Results and discussion

The dependence of shear strength on bonding temperature and bonding time is illustrated in Figs. 1 and 2, respectively. As the bonding temperature increases from 280 to 380 °C at bonding time of 3 min, the average bonding strength decreases from 9.9 to 1.6 MPa. As is shown in Fig. 2, the bonding strength decreases obviously with the increase of bonding time at bonding temperature of 280 °C. The highest average shear strength of 11 MPa is obtained at bonding temperature of 280 °C and bonding time of 1 min.

The error bars are included in Figs. 1 and 2. Each error bar was calculated from 10 test dies (5 mm × 5 mm) at least. Much smaller errors can be found for 380 °C/3 min in Fig. 1 and 280 °C/50 min in Fig. 2 and the errors vary largely with bonding conditions. It seems that the errors cannot be solely explained as statistical deviation due to limited number of test dies or simply related to measurement equipment or operation variation. We suppose that the errors in Figs. 1 and 2 are related to the ununiformity of the whole wafer bonding. It is obvious that the errors are larger for higher average shear strength results in both Figs. 1 and 2. For 280 °C/1 min bonding shown in Fig. 2, shear strength of some dies can be as high as 34.3 MPa, while that of some other dies is as small as 3 MPa. The results clearly show that with proper low thermal budget, we can achieve higher average bonding strength, while the whole wafer bonding strength ununiformity is more noticeable. To deeply understand the change of bonding strength and errors with bonding conditions, the analysis of the bonding mechanism is necessary.

An intensive study is made on the morphology of Sn film in order to investigate the underlying mechanism. After the shear test, the Sn layer is observed by SEM and

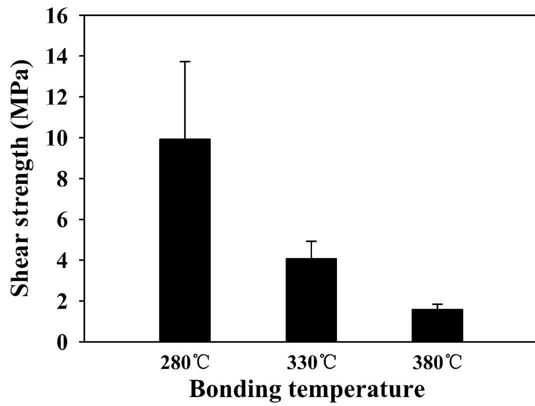

Fig. 1 Dependence of shear strength on bonding temperature. The bonding time is 3 min

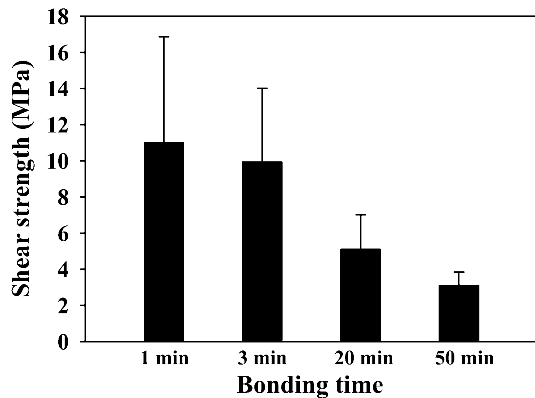

Fig. 2 Dependence of shear strength on bonding time. The bonding temperature is 280 °C

the images are shown in Fig. 3. Figure 3a shows that Sn layer is continuous with almost no voids. Figure 3b shows small voids in the Sn layer. Figure 3c shows several voids larger than 10 µm in Sn layer, which can be attributed to the melting of Sn layer during bonding. In Fig. 3d, the Sn layer becomes discontinuous and shows a complex and labyrinth-like pattern, which obviously indicates the melting of Sn layer. The microstructure illustrated in Fig. 3e–f shows deteriorated Sn film as well. The pattern of Sn layer in (e)–(f) is similar as that in (d). These SEM images show that the Sn layer structure seriously deteriorates with the increase of bonding temperature or bonding time.

It is obvious that the deteriorated Sn film with many voids decreases the effective bonding area. The voids in Sn layer and serious deterioration of Sn layer result from dewetting of molten Sn on Al surface during bonding. When a liquid layer is on the surface of a non-wetted solid, the liquid film is not stable and tends to expose voids due to dewetting, as discussed by Seemann et al. (2001).

The molten Sn flow driven by dewetting can be schematically illustrated in Fig. 4. In this model, it is assumed that the Al surface is flat, and there is no slip between molten Sn and Al surface. The fluid velocity profile is supposed to be the form shown in Fig. 4.

In consideration of incompressible, steady, two-dimensional laminar, viscous molten Sn flow between two wafers, we obtain

$$-\mu \frac{\partial^2 V_x}{\partial y^2} = -\frac{\partial \rho}{\partial x} \tag{1}$$

where μ is the absolute viscosity of the fluid, V_x is the velocity of the fluid, and ρ is the pressure in the fluid at x. The following formula can be achieved:

$$R = \sqrt{\frac{ht\gamma cos\theta}{3\mu}} \tag{2}$$

where R is the radius of the void, h is the distance between Al layers, and θ is the contact angle. Equation 2 indicates that R increases with Sn flow time. The results in Fig. 3a–f can be explained as that voids enlarge as bonding time increases, and large voids merge with each other, resulting in a complex and labyrinth-like structure. Figure 3b–d shows the enlargement of voids in Sn film by increasing the bonding temperature. According to Rozhitsina et al. (2011), the viscosity of molten Sn decreases as temperature increases and thus the increase of temperature also induces void elongation according to Eq. 2.

The adhesion energy between metal and metal can be characterized by the contact angle presented by researchers such as Murr (1981). The Al/Sn adhesion energy can be given as:

$$\mathrm{W}_{Ad} = \sigma_{Sn}(1 + cos\theta) \tag{3}$$

where σ_{Sn} is the surface energy of Sn, θ is the contact angle. By careful observation through SEM of the debonded samples, we found that the contact angle of Sn island is larger than 90 degree. This indicates that the melting of Sn during bonding may decrease the adhesion energy due to dewetting.

Figure 3a, b show small voids, which indicates less damaged and more continuous Sn layers after bonding. On the other hand, even there is no obvious voids in Sn layers, it is still possible that the dewetting of molten Sn can largely weaken the adhesion strength between Sn layer and Al layer in some area of the wafer because of ununiformity of interface morphology across the wafer or impurity contamination in some area. That's why the errors are obvious for higher average shear strength such as the shear strength of 280 °C/1 min and 280 °C/3 min shown in Figs. 1 and 2.

From above analysis, the deterioration of bonding strength is summarized as follows. Firstly, the void caused

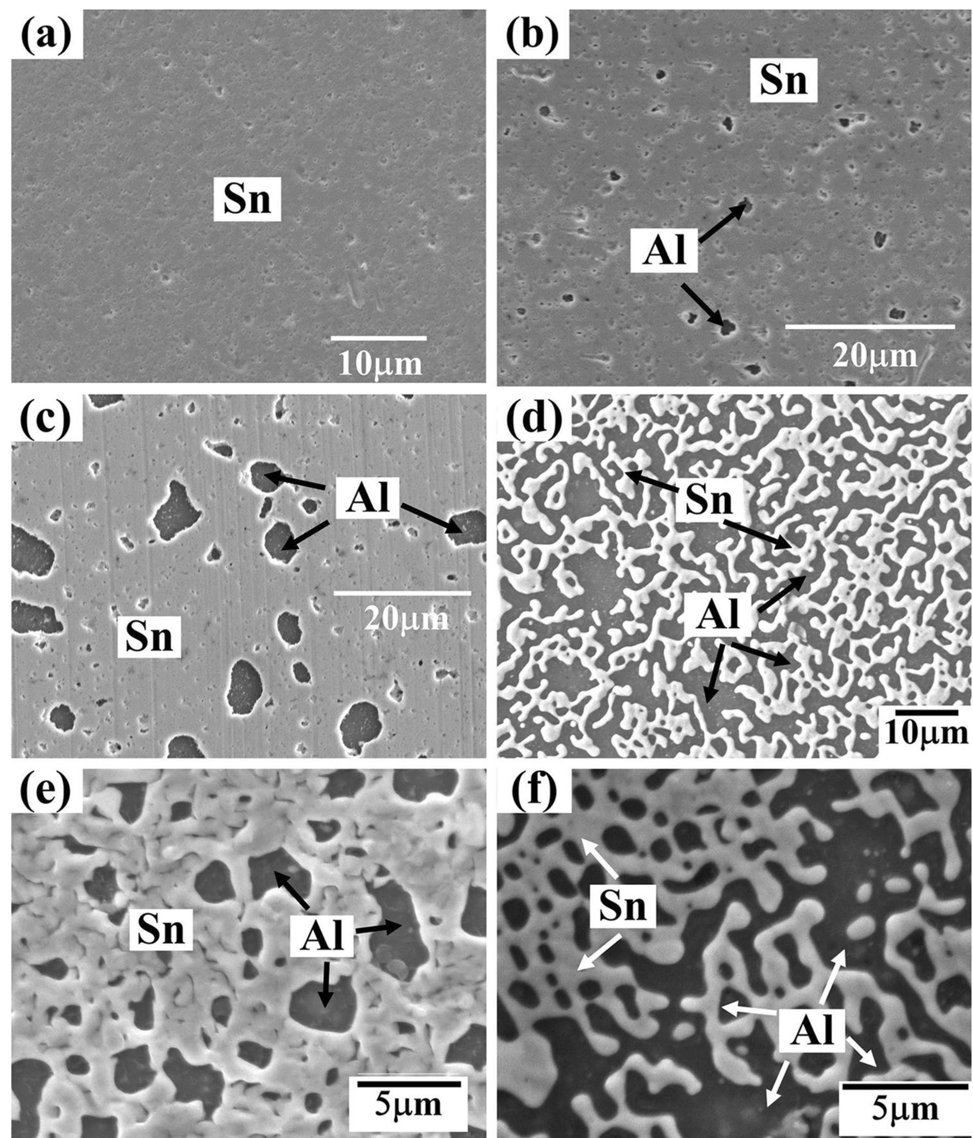

Fig. 3 SEM image of Sn layer. The serial number (**a**–**f**) correspond to bonding experiment No. 1–6, respectively

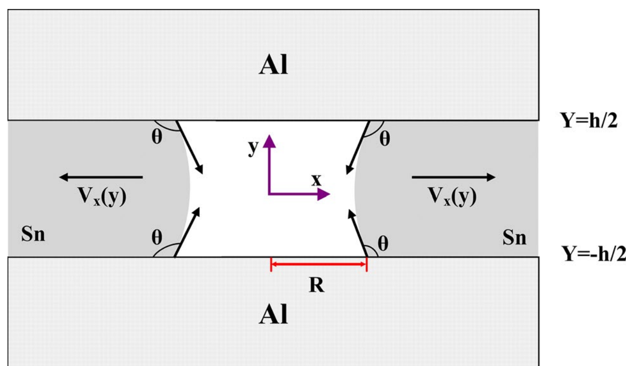

Fig. 4 Schematic diagram of molten Sn flow driven by dewetting

by dewetting would largely decrease the bonded area. Secondly, Al/Sn adhesion strength is reduced due to dewetting confirmed by contact angle observation. With proper low thermal budget, i.e. low bonding temperature and short bonding time, bonding strength can be improved, as is illustrated in Figs. 1 and 2. This can be attributed to reduced radius of the void in Sn layer and possible decrease of adhesion energy.

4 Conclusion

This paper researches silicon wafer bonding with Al and Sn thin film under low bonding temperature and short bonding time for application of 3D packaging and heterogeneous integration with small thermal budget. At bonding temperature of 280 °C, the average shear strength of 11 MPa can be achieved at bonding time of 1 min. Average shear strength decreases dramatically with increase of bonding temperature or bonding time.

Acknowledgments The work presented is funded by Major State Basic Research Development Program of China (Project No. 2015CB057201), National Science and Technology Major Project of China (Project No. 2013ZX02501), and National Science and Technology Major Project of China (Project No. 2009ZX02038-02). Zhiyuan Zhu would like to thank the China Scholarship Council for Fellowship support.

References

Chanchani R, Nordquist CD, Olsson RH, Peterson T, Shul R, et al (2011) A new wafer-level packaging technology for MEMS with hermetic micro-environment. Proceedings of IEEE 61st Electronic Components and Technology Conference, Lake Buena Vista, FL, pp 1604–1609. doi:10.1109/ECTC.2011.5898725

Chang JY, Lin LW (2010) MEMS packaging technologies and applications. International Symposium on VLSI Design Automation and Test, Hsin Chu, pp 126–129. doi:10.1109/VDAT.2010.5496707

Fischer A, Forsberg F, Lapisa MA, Roxhed N, Stemme G, et al (2012) Heterogeneous integration for optical MEMS. Proceedings of 23rd Annual Meeting of the IEEE Photonics Society, Denver, CO, pp 487–488. doi:10.1109/PHOTONICS.2010.5698973

Lapisa M, Steme G, Niklaus F (2011) Wafer-level heterogeneous integration for MOEMS, MEMS, and NEMS. IEEE J Sel Top Quant Electron 17:629–644. doi:10.1109/JSTQE.2010.2093570

Lin HC, Chang KL, Hsieh KC, Cheng KY, Wang WH (2002) Metallic wafer bonding for the fabrication of long-wavelength vertical-cavity surface-emitting lasers. J Appl Phys 92:4132. doi:10.1063/1.1502200

Lin H, Stevenson JTM, Gundlach AM, Dunare CC, Walton AJ (2008) Direct Al–Al contact using low temperature wafer bonding for integrating MEMS and CMOS devices. Microelectron Eng 85:1059–1061. doi:10.1016/j.mee.2008.01.054

Malik N, Schjølberg-Henriksen K, Poppe E, Taklo MMV, Finstad TG (2014) Al-Al thermocompression bonding for wafer-level MEMS sealing. Sensors Actuators A 211:115–120. doi:10.1016/j.sna.2014.02.030

Malik N, Schjølberg-Henriksen K, Poppe E, Taklo MMV, Finstad TG (2015) Impact of SiO_2 on Al–Al thermocompression wafer bonding. J Micromech Microeng 25:035025. doi:10.1088/0960-1317/25/3/035025

Murr LE (1981) Surfaces and interfaces in ceramic and ceramic-metal systems. In: Pask J et al (eds) The series materials science research. Plenum Press, New York, pp 107–110

Rozhitsina EV, Gruner S, Kaban I, Hoyer W, Sidorov VE et al (2011) Dynamic viscosities of pure tin and Sn–Ag, Sn–Cu, and Sn–Ag–Cu eutectic melts. Russian Metall (Metally) 2011:118–121

Saha R, Fritz N, Bidstrup-Allen SA, Kohl PA (2013) Packaging-compatible wafer level capping of MEMS devices. Microelectron Eng 104:75–84. doi:10.1016/j.mee.2012.11.010

Seemann R, Herminghaus S, Jacobs K (2001) Gaining control of pattern formation of dewetting liquid films. J Phys Condens Matter 13:4925

Tana CS, Lim DF, Ang XF, Wei J, Leong KC (2012) Low temperature Cu–Cu thermo-compression bonding with temporary passivation of self-assembled monolayer and its bond strength enhancement. Microelectron Reliab 52:321–324. doi:10.1016/j.microrel.2011.04.003

Yun CH, Martin JR, Tarvin EB, Winbigler JT (2008) Al to Al wafer bonding for MEMS encapsulation and 3-D interconnect. Proceedings of IEEE 21st International Conference on Micro Electro Mechanical Systems, Tucson, AZ, pp 990–993. doi:10.1109/MEMSYS.2008.4443780

Zhu ZY, Yu M, Tian DY, Zhu YW, Wang PQ et al (2013) Aluminum-coated silicon wafer bonding with tin intermediate layer. J Micro/Nanolith MEMS MOEMS 12:010101. doi:10.1117/1.JMM.12.1.013012